Atmos. Meas. Tech. Discuss., 3, 469–499, 2010
www.atmos-meas-tech-discuss.net/3/469/2010/

Atmospheric Measurement Techniques Discussions

This discussion paper is/has been under review for the journal Atmospheric Measurement Techniques (AMT). Please refer to the corresponding final paper in AMT if available.

Auto MAX-DOAS measurements around entire cities: quantification of NO_x emissions from the cities of Mannheim and Ludwigshafen (Germany)

O. Ibrahim[1], R. Shaiganfar[1], R. Sinreich[2,3], T. Stein[2,4], U. Platt[2], and T. Wagner[1]

[1]Max-Planck-Institute for Chemistry, Mainz, Germany
[2]Institute for Environmental Physics, University of Heidelberg, Germany
[3]now at: University of Colorado at Boulder, USA
[4]now at: Ernst & Young, Luxembourg, Luxembourg

Received: 2 February 2010 – Accepted: 2 February 2010 – Published: 11 February 2010

Correspondence to: T. Wagner (thomas.wagner@mpch-mainz.mpg.de)

Published by Copernicus Publications on behalf of the European Geosciences Union.

Abstract

We present Auto Multi-Axis (MAX-) DOAS observations of tropospheric NO_2 carried out on circles around the cities of Mannheim and Ludwigshafen (Germany) on 24 August 2006. Together with information on wind speed and direction, the total emissions of the encircled source(s) can be quantified from these measurements. In contrast to recent similar studies based on of zenith scattered sun light (elevation angle of 90°), we use a MAX-DOAS instrument mounted on a car, which observes scattered sun light under different elevation angles (here 45°, and 90°). Compared to simple zenith sky observations, MAX-DOAS observations have higher sensitivity and avoid systematic offsets in the determination of the vertically integrated trace gas concentration. Auto MAX-DOAS observations are especially well suited for the determination of the total emission of extended emission sources (e.g. whole cities), for which typically no sharply defined plumes are formed. In such cases, the trace gas concentrations can be rather small and thus even small systematic offsets in the observed integrated tropospheric trace gas concentration can have a large effect on the determined total emissions. However, such measurements are still affected by several uncertainties which need to be further investigated and minimised. The largest error source is probably the variability and imperfect knowledge of the wind field. In addition – depending on the trace species observed – also chemical transformations between the emission sources and the measurement location have to be considered. In this study we use local observations within the encircled area to quantify and correct these errors. From our observations we derive a total NO_x emission from the Mannheim/Ludwigshafen area of $(7.2\pm1.7)\times10^{24}$ molecules/s (or 17350±4100 t, calculated with the mass of NO_2), which is in surprisingly good agreement with existing emission estimates.

AMTD

3, 469–499, 2010

1 Introduction

The precise knowledge of the emissions of natural and anthropogenic trace gases (e.g. pollutants or greenhouse gases) is important for many applications. Emission estimates are used as input to atmospheric chemistry and transport models. By varying the strengths of the emission sources in the model, it is e.g. possible to predict which emission reductions would have the strongest impact on air quality in a given area. Similar arguments hold for the emission inventories of greenhouse gases, which are important input in models predicting future climate. Accurate knowledge of the emission strengths from different sources is especially important to quantify the influence of anthropogenic emissions in comparison to natural emissions.

Usually, emission inventories are built using bottom-up strategies. Emission strengths of individual sources are quantified and summed up according to the frequency of the respective source type. Uncertainties of the calculated emission inventories result from both errors in the estimate of the number of individual sources and errors in the emission strength of individual sources.

An alternative to bottom-up emission inventories are top-down emission inventories. They are based on measurements of the atmospheric concentration of a pollutant, which is then related to the emission strength of an individual source or an integrated source strength within a specified area. For the determination of the emission strength of an observed trace gas additional knowledge on the atmospheric transformation processes (transport and chemistry) is required. Depending on the complexity of the emission source (e.g. a point source or a mixture of different sources with different spatio-temporal emission patterns) and the information content of the measurement (e.g. point measurements at fixed locations, or satellite observations), either simple assumptions (e.g. on the atmospheric lifetime and wind fields), or complex inverse models are required.

In this study we estimate the total urban NO_x emissions from Auto MAX-DOAS observations performed on circular driving routes around complete cities. This method

AMTD
3, 469–499, 2010

was recently introduced and applied to determine emissions of SO_2, NO_2 and HCHO (Johansson et al., 2008, 2009; Rivera et al., 2009). In contrast to these zenith sky observations we use MAX-DOAS observations, which have several advantages: first because of the slant path through the troposphere they have a higher sensitivity for tropospheric trace gases. Second, the results of MAX-DOAS observations are less affected by light path modifications caused by multiple scattering in thick clouds (see e.g., Johansson et al., 2008), because the measurements at different elevation angles are affected by such clouds in a similar way. Third, MAX-DOAS observations allow to determine the vertically integrated tropospheric trace gas concentration (vertical column density, VCD) above the instrument location without systematic biases (Wagner et al., 2010). In contrast, from zenith looking instruments only the difference of the tropospheric VCD compared to a reference measurement can be determined. This complicates the interpretation of the measurements especially in cases when emission sources are not completely encircled (Johansson et al., 2009). MAX-DOAS observations allow the determination of absolute tropospheric VCDs, which is also important for the quantitative comparison with model results and for the validation of satellite observations.

In addition to the inherent vertical integration of the tropospheric trace gas concentration by MAX-DOAS observations, a horizontal integration can be carried out if MAX-DOAS observations are performed from aircrafts or cars. Such observations eventually allow to determine the complete flux F of trace gas molecules across the area span given by the driving route $\vec{s}$ and the vertical (see Fig. 1). For that purpose the knowledge of the wind speed and direction is required:

$$F = \int_S \mathrm{VCD}(\vec{s}) \cdot \vec{\boldsymbol{W}}(\vec{s}) \cdot d\vec{s} \tag{1}$$

Here $\vec{\boldsymbol{W}}\left(\vec{s}\right)$ is the average wind vector within the trace gas layer. The integral is evaluated along the driving route $\vec{s}$.

AMTD
3, 469–499, 2010

We carry out Auto MAX-DOAS measurements along closed driving routes around large emissions sources, e.g. whole cities (Fig. 2). If the emission sources are completely encircled, the total flux entering the encircled area (on the side from which the wind blows) as well as the total flux leaving the encircled area (at the opposite side, see Fig. 2) can be determined (see also Johansson et al., 2008). In simple cases, the difference between both fluxes yields the integrated total emission of the encircled area. To determine the total flux F_{total} of the encircled area the integral in Eq. (1) has to be evaluated along the complete circle around the area of interest:

$$F_{\text{total}} = \int_A \text{div}(\text{VCD})\, dA = \oint \text{VCD}(\vec{s}) \cdot \vec{\boldsymbol{W}}(\vec{s}) \cdot d\vec{s} \quad (2)$$

It should be noted that for the complete surrounding of extended areas the driving period is typically between a few ten minutes and more than one hour. Thus temporal variations on time scales below that period can not be resolved and the resulting emission estimates therefore are averages over the period of the observations. Two main effects complicate the determination of the total emission and have to be taken into consideration:

A) Transport by wind

In the simplest case, a wind field with constant speed and direction is present over the complete area of interest, and the wind speed is also high enough that the transport across the encircled area is fast compared to the atmospheric lifetime of the trace gas. In more complicated cases, the wind speed is low and varies with time and location within the encircle area. In such cases, emission estimates are difficult and might only be possible with the additional use of atmospheric model simulations. A further general problem is caused by the fact that the wind speed usually increases with altitude (also the direction changes systematically), but the vertical distribution of the observed trace gas is usually not well known. Thus assumptions on the vertical distribution and appropriate wind speed have to be made.

AMTD
3, 469–499, 2010

B) Chemical transformations

Chemical transformations and deposition processes change the trace gas abundance after the emission process. Depending on the speed, two cases can be distinguished. First, rapid chemical reactions can change the partitioning of the emitted species. In this study, MAX-DOAS observations of NO_2 are investigated, while most of the NO_2 was primarily emitted as NO. The partitioning of both species depends on the ozone concentration and the NO_2 photolysis rate. In order to quantify the total NO_x (NO_2+NO) emissions, the so called Leighton ratio (L=[NO]/[NO_2]) has to be known (or assumed). Second, the atmospheric concentration of the emitted species can be changed by processes, which are slow compared to the transport time between the emission source and the location of the measurement. Thus, the measured trace gas concentration represents only a fraction of the emitted trace gas abundance. These destruction processes are usually described by an exponential decrease with an e-folding lifetime τ, after which the trace gas concentration is reduced to a fraction $1/e$ of the initial value. It should be noted that in cases of substantial trace gas destruction between the emission source and the location of the measurement (short atmospheric lifetime compared to the transport time), also the spatial distribution of the emission sources within the encircled area becomes important.

These potential error sources are discussed in detail and quantified for the Auto MAX-DOAS measurements presented in this study (see Sect. 4).

The paper is structured as follows: in Sect. 2 the MAX-DOAS method is briefly introduced and the performed Auto MAX-DOAS measurements are described. Section 3 provides details on the different steps of the data analysis. In Sect. 4 the results of our measurements are presented and the uncertainties caused by the different error sources are discussed and quantified.

2 MAX-DOAS observations

In recent years Multi-Axis-Differential Optical Absorption Spectroscopy (MAX-DOAS) observations have become a widely and successfully used technique for the remote sensing of tropospheric trace gases and aerosols. MAX-DOAS instruments observe scattered sun light under different slant viewing angles, which make them especially sensitive to tropospheric trace gases and aerosols (e.g., Hönninger et al., 2002, 2004a,b; Leser et al., 2003; Van Roozendael et al., 2003; Wittrock et al., 2004; Wagner et al., 2004; Sinreich et al., 2005, 2007; Heckel et al., 2005; Frieß et al., 2006; Fietkau et al., 2007; Theys et al., 2007; Brinksma et al., 2008; Wagner et al., 2007a,b; Irie et al., 2009). From MAX-DOAS observations, vertical profiles of tropospheric trace gases and aerosol extinction can be retrieved yielding up to a few pieces of information, with the highest vertical resolution close to the surface (see e.g., Theys et al., 2007). However, profile retrievals are typically restricted to MAX-DOAS measurements made at fixed locations and under cloud free conditions. For MAX-DOAS observations made from moving platforms, horizontal gradients of the trace gas concentration often prevent a meaningful profile retrieval. In addition, unlike ship measurements, for car measurements the observations at low elevation angles are usually affected by obstacles (e.g. trees or houses) in the field of view. Thus from mobile MAX-DOAS observations usually only the (absolute) tropospheric VCD is determined.

2.1 Determination of the tropospheric VCD

For the retrieval of the tropospheric VCD, typically observations at rather high elevation angles (>about 10°) are used. For such elevation angles the effects of atmospheric aerosols are rather small and the atmospheric light paths can be geometrically well approximated (Brinksma et al., 2008; A. Richter, personal communication, 2005). In addition, the retrieval of tropospheric VCDs is usually even possible in the presence of clouds (at least for trace gases located below the cloud base).

For the analysis of MAX-DOAS observations it is usually assumed that the concen-

tration field does not change during the time period needed for the observations at the different elevation angles. This assumption is roughly valid for MAX-DOAS observations made at fixed locations. In contrast, mobile MAX-DOAS observations are typically strongly affected by horizontal concentration gradients of air masses probed along the driving route. For these platforms, the usual way of the MAX-DOAS data analysis can thus lead to large errors, in extreme cases even negative concentrations might be obtained. Recently a technique was developed which overcomes this problem and allows to determine absolute tropospheric VCDs along the driving route (Wagner et al., 2010).

2.2 Auto MAX-DOAS instrumentation for the Mannheim/Ludwigshafen measurements

The Mini-MAX-DOAS instrument is a fully automated, light weighted spectrometer (13 cm×19 cm×14 cm) designed for the spectral analysis of scattered sunlight (e.g., Bobrowski et al., 2003; Hönninger et al., 2004). It consists of a sealed aluminium box containing the entrance optics, a fibre coupled spectrograph and the controlling electronics. A stepper motor mounted outside the box rotates the whole instrument to control the elevation of the viewing angle (angle between the horizontal and the viewing direction). The entrance optics consists of a quartz lens of focal length f=40 mm coupled to a quartz fibre bundle which leads the collected light into the spectrograph (field of view is ~1.2°). The light is dispersed by a crossed Czerny-Turner spectrometer (USB2000, Ocean Optics Inc.) with a spectral resolution of 0.7 nm over a spectral range from 320–460 nm. A one-dimensional CCD (Sony ILX511, 2048 individual pixels) is used as detector. Before the signal is transferred to the 12 bit analog-to-digital converter, an electronic offset is added. After conversion, the signal is digitally transmitted to a laptop computer via one USB cable and stored for subsequent analysis.

For the mobile measurements the Mini-MAX-DOAS instrument was mounted on the top of a car (Auto MAX-DOAS) with the telescope pointing in driving direction and was powered by the 12 V car battery. The rest of the set-up was inside the car and both parts were connected via two electric cables. The measurements are controlled from

a laptop using the DOASIS software (Kraus, 2004).

On 24 August 2006, measurements were carried out around the Mannheim-Ludwigshafen industrial/urban area. The sequence of elevation angles was chosen to: 45°, 45°, 45°, 45°, 90°, and the duration of an individual measurement was about 20–25 s.

3 Data analysis

The measured spectra are analysed using the DOAS method (Platt and Stutz, 2008). A wavelength range of 415–435 nm was selected for the analysis. Several trace gas absorption cross sections (NO_2 at 297 K (Vandaele et al., 1998), H_2O at 300 K (Rothmann et al., 2005), O_4 at 296 K (Greenblatt et al., 1990), and O_3 at 243 K, Bogumil et al., 2003) as well as a Fraunhofer reference spectrum, a Ring spectrum (calculated from the Fraunhofer spectrum) and a polynomial of second order were included in the spectral fitting process using the WinDOAS software (Fayt and van Roozendael, 2001). The wavelength calibration was performed based on a high resolution solar spectrum (Kurucz et al., 1984). The output of the spectral analysis is the slant column density (SCD), the integrated trace gas concentration along the light path through the atmosphere. Following to the retrieval technique of Wagner et al. (2010) the tropospheric NO_2 VCD is determined from each observation made at 45° elevation angle using the zenith measurement of the respective sequence. In the retrieval process, tropospheric air mass factors (AMF) are needed, for which the geometric approximation is used:

$$\mathrm{AMF}(\alpha) = 1/\sin(\alpha) \quad (3)$$

Depending on the aerosol load and on the vertical distribution of the trace gas, the geometrical approximation for the tropospheric AMF can deviate to some degree from the true value. We investigated these deviations using the Monte Carlo radiative transfer model TRACY-2 (Wagner et al., 2007; Deutschmann and Wagner, 2008) and found that for aerosol loads with optical depth <0.5 for surface-near trace gases (<200 m)

AMTD
3, 469–499, 2010

the errors of the geometrical approximation are typically below 15%. In the presence of clouds the uncertainties can in principle become larger. However, especially for the part of the trace gas profile below the cloud (e.g. freshly emitted NO_x) the geometrical approximation is in general a very good choice, because the lower boundary of the cloud acts as well defined illumination source and scattering events below the cloud (within the trace gas layer) become less important.

The total error of the tropospheric NO_2 VCD is estimated from the typical fit residual and the uncertainty of the geometric approximation to $>3\times10^{15}$ molecules/cm^2 or >15%.

4 Results and discussion

Results of the Auto MAX-DOAS observations made on trips around the cities of Ludwigshafen and Mannheim (Southern Germany, see Fig. 3) on 24 August 2006 are shown in Figs. 4 and 5. The sky was mainly overcast and temperatures were around 20° C. Both cities were surrounded in four successive "circles" with approximate extensions of 26 km in north-south direction and 18 km in east-west direction. During these circles, a repeating pattern with high and low tropospheric NO_2 VCDs was found. In general the highest NO_2 VCDs were measured in the north-east corner, which can be directly related to the prevailing wind direction on that day (mainly from south-west). However, not exactly the same patterns are obtained for the different circles reflecting the variation of emissions as well as wind speed and direction.

From the MAX-DOAS observations the integrated NO_x emission within the encircled area can in principle be calculated according to Eq. (2). However, to account for the finite atmospheric lifetime and for the partitioning between NO and NO_2, two corrections have to be applied to Eq. (2):

$$F_{NO_x} = c_L \cdot c_\tau \cdot F_{NO_2} = c_L \cdot c_\tau \cdot \oint_S \mathrm{VCD}_{NO_2}(\vec{s}) \cdot \vec{\boldsymbol{W}}(\vec{s}) \cdot d\vec{s} \quad (4)$$

AMTD
3, 469–499, 2010

Here c_L is a correction factor which accounts for the partitioning of NO_x into NO and NO_2, which is typically expressed as Leighton ratio (L=[NO]/[NO_2]). c_τ is a correction factor which accounts for the destruction of NO_x while it is transported from the emission sources to the locations of the measurements.

In the following sub-sections the three terms of Eq. 4 are determined separately and applied to the measurements on 24 August 2006.

4.1 Integration of the tropospheric NO_2 flux along the driving route

In this section the integral of Eq. (4) is evaluated for the MAX-DOAS measurements around the cities of Mannheim and Ludwigshafen. Because of the finite integration time of the individual spectra, the integral is substituted by a sum which is evaluated for all observations made at 45° elevation during the individual circles:

$$F_{NO_2} = \sum_i \mathrm{VCD}_{NO_2}(\vec{s}_i) \cdot \vec{W}(\vec{s}_i) \cdot \Delta\vec{s}_i = \sum_i \mathrm{VCD}_{NO_2}(\vec{s}_i) \cdot W(\vec{s}_i) \cdot \sin(\beta)(\vec{s}_i) \cdot \Delta s_i \quad (5)$$

The distance between two measurements Δs_i is the geometric difference between the locations at the beginning of two successive measurements. For the wind direction and wind speed W constant values for all measurements during the respective circle were assumed. They were calculated from half hour averages at three meteorological stations within the encircled area: Mannheim south, Mannheim center, Mannheim north (http://mnz.lubw.baden-wuerttemberg.de/messwerte/aktuell/, the locations are indicated in Fig. 5). Also the angles $\beta(\vec{s}_i)$ between the driving route and the wind direction were calculated in discrete steps (the angle of the driving route was determined according to the starting points of two successive spectra). The average wind speeds and directions are listed in Table 1.

As an example, Fig. 6 shows the individual terms of the sum in Eq. (5) for the fourth circle on 24 August 2006. In the top panel the tropospheric NO_2 VCD is shown. The second panel shows the length of the driving route for the individual measurements (the difference of the instrument position between the start of two consecutive spectra). The

AMTD
3, 469–499, 2010

path length varies with the driving speed. In addition, according to the sequence of elevation angles systematically different path lengths between successive measurements are also found. Larger distances occur for the end of an elevation sequence because of the gap during the record of the zenith spectrum. In addition, also some time is needed to change the elevation angle. The third panel shows the sine of the angle between the driving route and the wind direction, respectively. The bottom panel shows the resulting tropospheric NO_2 flux above the driving route for the segment between two measurements taking into account also the wind speed (assumed to be constant, see Table 1). According to the relative orientation of the driving direction and wind direction, the NO_2 flux is either positive or negative. The high positive values at the beginning of the circle indicate the main emissions from the Mannheim/Ludwigshafen area. At the end of the circle both substantial negative and positive fluxes occur. They are probably caused by emissions from the city of Speyer south of the encircled area. They first enter and then leave the encircled area at the south-west edge (see Fig. 5). Besides this example, the influx (negative flux) of NO_2 into the encircled area is typically rather small. Summing-up the NO_2 fluxes along the driving route, yields a total emission of 5.8×10^{24} molecules/s NO_2. In Table 2 also the results for the other cycles are shown.

The uncertainty of the derived total emission is dominated by the variation and the imperfect knowledge of the wind field within the encircled area (see also discussion in Johansson et al., 2008). Three main uncertainties can be distinguished:

4.1.1 Errors caused by variations of the wind speed

We estimate errors caused by variations of the wind speed from the standard deviation of the wind speed at the different stations within the time of the measurements (see Table 1). In principle, fluctuations of the wind speed should cancel each other, and the knowledge of the average wind speed should be sufficient for the determination of the total emissions. However, this would only be true for short fluctuations and long measurement duration. If the wind speed changes systematically during the measurement period, the associated inhomogeneities of the wind field can lead to an over- or

AMTD
3, 469–499, 2010

underestimation of the total emissions, depending on the details of the distribution of individual emission sources within the encircled area. The resulting error is difficult to quantify without complete knowledge of the wind field and the distribution of emission sources. Here we estimate the relative error of the determined NO_2 emission associated with inhomogeneities of the wind field using half of the standard deviation (see Table 2).

4.1.2 Errors caused by uncertainties of the wind direction

Especially for measurements with the average wind direction almost parallel to parts of the driving route (e.g. as in circle 2) the precise knowledge of the wind direction becomes especially important. We estimated the associated errors by varying the wind direction by ±20° (see Table 2). For most circles, the errors are rather small, typically <15%. However, for the second circle (with the average wind direction almost parallel to larger parts of the driving route) the error reaches up to 60%.

4.1.3 Errors caused by the vertical variation of the wind

The wind speed and direction usually depend systematically on altitude with higher wind speeds at higher altitudes. Thus surface wind data typically underestimate the effective wind speed relevant for the NO_2 layer. According to Eq. (2) this directly leads to an underestimation of the determined NO_2 emissions. Here we apply no correction for this effect, because no wind profile data are available and also the vertical distribution of the NO_2 concentration is unknown. However, since most emission sources are located at the surface, it can be assumed that most of the freshly emitted NO_x should be present close to the surface (exceptions are e.g. power plants). Thus the resulting underestimation should be small (at least compared to other uncertainties).

We want to point out that our current way of estimating the errors associated to variations and missing knowledge of the wind field is rather crude and should be improved in future investigations (e.g. by using higher resolved wind data from measurements

AMTD
3, 469–499, 2010

and/or model simulations). Nevertheless, our current error estimate takes into account the most important errors caused by inhomogeneities of the wind field in a semi quantitative way.

4.2 Errors caused by chemical transformations

4.2.1 Estimation of the NO_x lifetime

In this section the effect of the finite atmospheric lifetime of NO_x (factor c_τ in Eq. 4) is estimated. The NO_x lifetime depends on meterological parameters (e.g. temperature) and on the photochemical state of the atmosphere, and is difficult to determine for the specific situation of our measurements. Thus we use an average value of 6 h for the NO_x lifetime which is derived from several experimental studies (Beirle et al., 2003, 2004a,b). According to the extension of the circles and the average wind speeds (Table 1) the time the air masses to cross the encircled area is about 2 h. Because most NO_x is emitted close to the center of the encircled area, we assume an effective transport time of 1 h. Within that duration the NO_x concentration decreases by about 15% for an assumed lifetime of 6 h. This results in a correction factor c_τ of 1.18. For assumed lifetimes of 4 and 8 h the correction factors would be 1.28 and 1.13, respectively. From this variation we estimate the uncertainty caused by the finite atmospheric liftetime of NO_x to about 10%.

4.2.2 Leighton ratio during the measurements

For the determination of the second correction factor c_L we use measurements of NO and NO_2 made at two meteorological stations (Mannheim North and Mannheim Center, see Fig. 7). For the period of the MAX-DOAS measurements Leighton ratios of about 0.35 were found. Thus we use a correction factor c_L of 1.35 to obtain to determine the total NO_x emissions. From the variation of the Leighton ratio during the time of our measurements we estimate the related uncertainties of the total emission to be about

10%.

4.3 Final results of NO_x emissions for the different circles

Table 3 summarises the total emissions and respective errors for the four circles. The calculated errors include the contributions associated with variations and imperfect knowledge of the wind field, NO_x lifetime, NO_x partitioning and retrieval of the tropospheric VCD.

The average of total NO_x emission calculated from the results of the four circles is $(7.2 \pm 1.7) \times 10^{24}$ molecules/s. This equals a NO_x emission of 0.55 kg/s (using the mass of NO_2).

4.4 Additional error sources

In some cases, additional complications can occur, e.g. if the NO concentrations are higher than the background ozone concentrations. Such situations might occur close to the stacks of power plants. Then the reaction of NO with ozone will eventually consume all available ozone, which prevents the further conversion of NO into NO_2. Only after additional ozone-rich air is mixed with the ozone-depleted air masses, the Leighton ratio expected for ozone-rich conditions can be established. For our measurements the ozone mixing ratio measured at the different stations (see Fig. 7) is found to be higher that the NO_x concentration. However, especially for emissions from the large power plant in the southern part of Mannheim these conditions might not be fulfilled and the measured NO_2 might underestimate the total NO_x emissions. Unfortunately, with our current knowledge this effect can not be quantified. Since the ozone concentrations increase during the day (Fig. 7), the possible underestimation should be smaller for the later measurements. The effect of suppressed NO to NO_2 conversion should be investigated in more detail in future studies.

AMTD
3, 469–499, 2010

5 Conclusions

We applied Auto MAX-DOAS observations for the determination of the total NO_x emissions from the Mannheim/Ludwigshafen industrial and urban area. This method is similar to that introduced by Johansson et al. (2008), but instead measuring scattered sun light under zenith sky observations, we use a MAX-DOAS instrument mounted on a car. MAX-DOAS observations measure scattered sunlight under various slant elevation angles and thus provide increased sensitivity for tropospheric species. Moreover, MAX-DOAS observations allow to determine the absolute value of the vertically integrated tropospheric trace gas concentration (tropospheric VCD). This makes the method especially well suited for observations of emissions from extended areas, for which the emission plumes might not be characterised by well defined and sharp gradients. Observations of the tropospheric VCD without systematic offsets are also important if the measurements are not performed on closed loops, but only along selected transects through the emission plume. In such cases Auto MAX-DOAS observations allow to quantify the absolute value of the total trace gas flux, which can be directly compared to model simulations or used for satellite validation.

Auto MAX-DOAS observations provide a rather simple and cheap method for the determination of total emissions of extended areas like complete cities. Thus they allow to check existing emission estimates with a completely independent method. As shown by Johansson et al. (2008) besides NO_2 also the emissions of other species like e.g. SO_2 and HCHO can be quantified. However, the accuracy of Auto MAX-DOAS should be further improved. Major uncertainties are caused by temporal and spatial variations of the wind field within the encircled area. Additional errors are related to chemical transformations between the emission source and the location of the measurement. In both cases more detailed information on the meteorological conditions and chemical composition would reduce the error sources. In this study we quantified the respective errors from in-situ observations within the encircled area.

On 24 August 2006 we performed Auto MAX.DOAS observations on 4 consecutive

AMTD
3, 469–499, 2010

circles around the cities of Mannheim and Ludwigshafen. The determined total emissions for these 4 circles range from 4.9×10^{24} to 9.2×10^{24} molecules/s with an average value of $(7.2\pm1.7)\times10^{24}$ molecules/s. If simply extrapolated to a complete year a value of 17350±4100 tons NO_x/yr (calculated with the mass of NO_2) is derived. This value compares well with existing emission estimates of both cities. For Ludwigshafen NO_x emissions of 7950 t/yr are reported for 2004 (Landesamt für Umwelt, 2008) and for Mannheim NO_x emissions of 10121 t/yr are reported for 2002 (Regierungspräsidium Karlsruhe, 2006). Both values sum up to 18 071 t/yr.

Acknowledgements. For the interpretation of our measurements we used information on meteorology and chemical composition from three in-situ monitoring stations of the city of Mannheim (http://mnz.lubw.baden-wuerttemberg.de/messwerte/aktuell).

The service charges for this open access publication
have been covered by the Max Planck Society.

References

Beirle, S., Platt, U., Wenig, M., and Wagner, T.: Weekly cycle of NO_2 by GOME measurements: a signature of anthropogenic sources, Atmos. Chem. Phys., 3, 2225–2232, 2003, http://www.atmos-chem-phys.net/3/2225/2003/.

Beirle, S., Platt, U., von Glasow, R., Wenig, M., and Wagner, T.: Estimate of nitrogen oxide emissions from shipping by satellite remote sensing, Geophys. Res. Lett., 31, L18102, doi:10.1029/2004GL020312, 2004a.

Beirle, S., Platt, U., Wenig, M., and Wagner, T.: Highly resolved global distribution of tropospheric NO2 using GOME narrow swath mode data, Atmos. Chem. Phys., 4, 1913–1924, 2004b, http://www.atmos-chem-phys.net/4/1913/2004/.

Bobrowski, N., Hönninger, G., Galle, B., and Platt, U.: Detection of bromine monoxide in a volcanic plume, Nature, 423, 273–276, 2003.

Brinksma, E. J., Pinardi, G., Braak, R., Volten, H., Richter, A., Schönhardt, A., van Roozendael, M., Fayt, C., Hermans, C., Dirksen, R. J., Vlemmix, T., Berkhout, A. J. C., Swart, D. P. J.,

Ötjen, H., Wittrock, F., Wagner, T., Ibrahim, O. W., de Leeuw, G., Moerman, M., Curier, R. L., Celarier, E. A., Knap, W. H., Veefkind, J. P., Eskes, H. J., Allaart, M., Rothe, R., Piters, A. J. M., and Levelt, P. F.: The 2005 and 2006 DANDELIONS NO_2 and Aerosol Validation Campaigns, J. Geophys. Res., 113, D16S46, doi:10.1029/2007JD008808, 2008.

Bogumil, K., Orphal, J., Homann, T., Voigt, S., Spietz, P., Fleischmann, O. C., Vogel, A., Hartmann, M., Bovensmann, H., Frerik, J., and Burrows, J. P.: Measurements of molecular absorption spectra with the SCIAMACHY pre-flight model: instrument characterization and reference data for atmospheric remote-sensing in the 230–2380 nm region, J. Photoch. Photobio. A, 157, 167–184, 2003.

Deutschmann, T. and Wagner, T.: TRACY-II users manual, http://joseba.mpch-mainz.mpg.de/Strahlungstransport.htm, last access: February, 2010, 2008.

Fayt, C. and Van Roozendael, M.: WinDOAS 2.1 software user manual, http://www.oma.be/BIRA-IASB/Molecules/BrO/WinDOAS-SUM-210b.pdf, last access: February, 2010, 2001.

Fietkau, S., Medeke, T., Richter, A., Sheode, N., Sinnhuber, B.-M., Wittrock, F., Theys, N., van Roozendael, M., and Burrows, J. P.: Ground-based measurements of tropospheric and stratospheric bromine monoxide above Nairobi (1° S, 36° E), Atmos. Chem. Phys. Discuss., 7, 6527–6555, 2007, http://www.atmos-chem-phys-discuss.net/7/6527/2007/.

Frieß, U., Monks, P. S., Remedios, J. J., Rozanov, A., Sinreich, R., Wagner, T., and Platt, U.: MAX-DOAS O_4 measurements: a new technique to derive information on atmospheric aerosols. (II) Modelling studies, J. Geophys. Res., 111, D14203, doi:10.1029/2005JD006618, 2006.

Greenblatt, G. D., Orlando, J. J., Burkholder, J. B., and Ravishankara, A. R.: Absorption measurements of oxygen between 330 and 1140 nm, J. Geophys. Res., 95, 18577–18582, 1990.

Heckel, A., Richter, A., Tarsu, T., Wittrock, F., Hak, C., Pundt, I., Junkermann, W., and Burrows, J. P.: MAX-DOAS measurements of formaldehyde in the Po-Valley, Atmos. Chem. Phys., 5, 909–918, 2005, http://www.atmos-chem-phys.net/5/909/2005/.

Hönninger, G. and Platt, U.: Observations of BrO and its vertical distribution during surface ozone depletion at alert, Atmos. Environ., 36, 2481–2490, 2002.

Hönninger, G., von Friedeburg, C., and Platt, U.: Multi axis differential optical absorption spectroscopy (MAX-DOAS), Atmos. Chem. Phys., 4, 231–254, 2004a, http://www.atmos-chem-phys.net/4/231/2004/.

Hönninger, G., Leser, H., Sebastian, O., and Platt, U.: Ground-based measurements of halogen oxides at the Hudson Bay by active long path DOAS and passive MAX-DOAS, Geophys. Res. Lett. 31, L04111, doi:10.1029/2003GL018982, 2004b.

Irie, H., Kanaya, Y., Akimoto, H., Iwabuchi, H., Shimizu, A., and Aoki, K.: Dual-wavelength aerosol vertical profile measurements by MAX-DOAS at Tsukuba, Japan, Atmos. Chem. Phys., 9, 2741–2749, 2009, http://www.atmos-chem-phys.net/9/2741/2009/.

Johansson, M., Galle, B., Yu, T., Tang, L., Chen, D., Li, H., Li, J. X., and Zhang, Y.: Quantification of total emission of air pollutants from Beijing using mobile mini-DOAS, Atmos. Environ., 42, 6926–6933, 2008.

Johansson, M., Rivera, C., de Foy, B., Lei, W., Song, J., Zhang, Y., Galle, B., and Molina, L.: Mobile mini-DOAS measurement of the outflow of NO_2 and HCHO from Mexico City, Atmos. Chem. Phys., 9, 5647–5653, 2009, http://www.atmos-chem-phys.net/9/5647/2009/.

Kraus, S. G.: DOASIS, A framework design for DOAS, Ph.D. thesis, University of Mannheim, , last access: February 2010.

Kurucz, R. L., Furenlid, I., Brault, J., and Testerman, L.: Solar flux atlas from 296 nm to 1300 nm, National Solar Observatory Atlas No. 1, Office of University publisher, Harvard University, Cambridge, 1984.

Landesamt für Umwelt, Luftreinhalte- und Aktionsplan Ludwigshafen: Fortschreibung 2007–2015, http://www.luwg.rlp.de/icc/luwg/nav/d20/binarywriterservlet?imgUid=d5a5ebba-f225-911a-3b21-7128749cab66&uBasVariant=11111111-1111-1111-1111-111111111111&isDownload=true, Landesamt für Umwelt, Wasserwirtschaft und Gewerbeaufsicht, Mainz, Germany, last access: February 2010, October 2008.

Leser, H., Hönninger, G., and Platt, U.: MAX-DOAS measurements of BrO and NO_2 in the marine boundary layer, Geophys. Res. Lett., 30(10), 1537, doi:10.1029/2002GL015811, 2003.

Platt, U. and Stutz, J.: Differential Optical Absorption Spectroscopy, Principles and Applications, Springer, Berlin, 2008.

Regierungspräsidium Karlsruhe: Luftreinhalte-/Aktionsplan für den Regierungsbezirk Karlsruhe, Teilplan Mannheim, http://www.mannheim.de/io2/download/webseiten/politik/aemter/fb63/dokumente/luftreinhalteplan.pdf, Regierungspräsidium Karlsruhe, Germany, last access: February 2010, March 2006.

Rivera, C., Sosa, G., Wöhrnschimmel, H., de Foy, B., Johansson, M., and Galle, B.: Tula in-

dustrial complex (Mexico) emissions of SO_2 and NO_2 during the MCMA 2006 field campaign using a mobile mini-DOAS system, Atmos. Chem. Phys., 9, 6351–6361, 2009, http://www.atmos-chem-phys.net/9/6351/2009/.

Rothman, L. S., Jacquemart, D., Barbe, A., Benner, D. C., Birk, M., Brown, L. R., Carleer, M. R., Chackerian Jr., C., Chance, K., Coudert, L. H., Dana, V., Devi, V. M., Flaud, J.-M., Gamache, R. R., Goldman, A., Hartmann, J.-M., Jucks, K. W., Maki, A. G., Mandin, J.-Y., Massie, S. T., Orphal, J., Perrin, A., Rinsland, C. P., Smith, M. A. H., Tennyson, J., Tolchenov, R. N., Toth, R. A., Vander Auwera, J., Varanasi, P., and Wagner, G.: The HITRAN 2004 molecular spectroscopic database, J. Quant. Spectrosc. Ra., 96, 139–204, 2005.

Sinreich, R., Frieß, U., Wagner, T., and Platt, U.: Multi axis differential optical absorption spectroscopy (MAX-DOAS) of gas and aerosol distributions, Faraday Discuss., 130, 135–164, doi:10.1039/b419274, 2005.

Sinreich, R., Volkamer, R., Filsinger, F., Frieß, U., Kern, C., Platt, U., Sebastián, O., and Wagner, T.: MAX-DOAS detection of glyoxal during ICARTT 2004, Atmos. Chem. Phys., 7, 1293–1303, 2007, http://www.atmos-chem-phys.net/7/1293/2007/.

Theys, N., Van Roozendael, M., Hendrick, F., Fayt, C., Hermans, C., Baray, J.-L., Goutail, F., Pommereau, J.-P., and De Mazière, M.: Retrieval of stratospheric and tropospheric BrO columns from multi-axis DOAS measurements at Reunion Island (21° S, 56° E), Atmos. Chem. Phys., 7, 4733–4749, 2007, http://www.atmos-chem-phys.net/7/4733/2007/.

Vandaele, A. C., Hermans, C., Simon, P. C., Carleer, M., Colin, R., Fally, S., Mérienne, M.-F., Jenouvrier, A., and Coquart, B.: Measurements of the NO_2 Absorption Cross-section from 42 000 cm^{-1} to 10 000 cm^{-1} (238–1000 nm) at 220 K and 294 K, J. Quant. Spectrosc. Ra., 59, 171–184, 1997.

Van Roozendael, M., Fayt, C., Post, P., Hermans, C., and Lambert, J.-C.: Retrieval of BrO and NO_2 from UV-Visible observations, in: Sounding the Troposphere from Space: a New Era for Atmospheric Chemistry, edited by: Borrell, P. M., Burrows, J. P., Platt,U., et al., Springer-Verlag, ISBN 3-540-40873-8, 2003.

Wagner, T., Dix, B., v. Friedeburg, C., Frieß, U., Sanghavi, S., Sinreich, R., and Platt, U.: MAX-DOAS O_4 measurements – a new technique to derive information on atmospheric aerosols. (I) Principles and information content, J. Geophys. Res., 109, D22205,

doi:10.1029/2004JD004904, 2004.
Wagner, T., Burrows, J. P., Deutschmann, T., Dix, B., von Friedeburg, C., Frieß, U., Hendrick, F., Heue, K.-P., Irie, H., Iwabuchi, H., Kanaya, Y., Keller, J., McLinden, C. A., Oetjen, H., Palazzi, E., Petritoli, A., Platt, U., Postylyakov, O., Pukite, J., Richter, A., van Roozendael, M., Rozanov, A., Rozanov, V., Sinreich, R., Sanghavi, S., and Wittrock, F.: Comparison of box-air-mass-factors and radiances for Multiple-Axis Differential Optical Absorption Spectroscopy (MAX-DOAS) geometries calculated from different UV/visible radiative transfer models, Atmos. Chem. Phys., 7, 1809–1833, 2007a, http://www.atmos-chem-phys.net/7/1809/2007/.
Wagner, T., Ibrahim, O., Sinreich, R., Frieß, U., von Glasow, R., and Platt, U.: Enhanced tropospheric BrO over Antarctic sea ice in mid winter observed by MAX-DOAS on board the research vessel Polarstern, Atmos. Chem. Phys., 7, 3129–3142, 2007b, http://www.atmos-chem-phys.net/7/3129/2007/.
Wagner, T., Ibrahim, O., Shaiganfar, R., and Platt, U.: Mobile MAX-DOAS observations of tropospheric trace gases, Atmos. Meas. Tech., 3, 129–140, 2010, http://www.atmos-meas-tech.net/3/129/2010/.
Wittrock, F., Oetjen, H., Richter, A., Fietkau, S., Medeke, T., Rozanov, A., and Burrows, J. P.: MAX-DOAS measurements of atmospheric trace gases in Ny-Ålesund – Radiative transfer studies and their application, Atmos. Chem. Phys., 4, 955–966, 2004, http://www.atmos-chem-phys.net/4/955/2004/.

Table 1. Wind data calculated from three stations (Mannheim center, south, north, see Fig. 5). For each cycle, the average and standard deviation of wind speed and direction are calculated.

Circle	Time	Wind direction (°) (wind from north is zero)	Wind speed (cm/s)
1	1, 10:30–12:00	239 (±44)	268±109
2	2, 11:30–13:00	265 (±17)	226±101
3*	3*, 13:00–14:30	223 (±18)	267±71
4	4, 13:30–15:00	219 (±14)	314±85

* L3 partly overlaps with L4, see Fig. 4

AMTD
3, 469–499, 2010

Table 2. Total NO_2 emissions for the different circles. Also shown are the relative errors related to variations and imperfect knowledge of the wind field.

Circle	Time	NO_2 Emissions (molecules/s)	Errors caused by uncertainties of the wind direction	Errors caused by inhomogeneities of the wind field	Total error
1	10:30–12:00	4.4×10^{24}	13%	21%	25%
2	11:30–13:00	3.1×10^{24}	60%	23%	64%
3*	12:30–14:00	4.1×10^{24}	10%	13%	17%
4	13:30–15:00	5.8×10^{24}	16%	14%	21%

* Partly overlaps with L4

Table 3. NO_x emissions from the encircled area after corrections for the lifetime and NO_x partitioning. The total error includes the sun of all error contributions (retrieval of the tropospheric VCD, wind field, NO_x lifetime, NO_x partitioning).

Circle	Time	NO_x Emissions (molecules/s)	Total error
1	10:30–12:00	7.0×10^{24}	32%
2	11:30–13:00	4.9×10^{24}	67%
3*	12:30–14:00	6.5×10^{24}	27%
4	13:30–15:00	9.2×10^{24}	29%

* Partly overlaps with L4

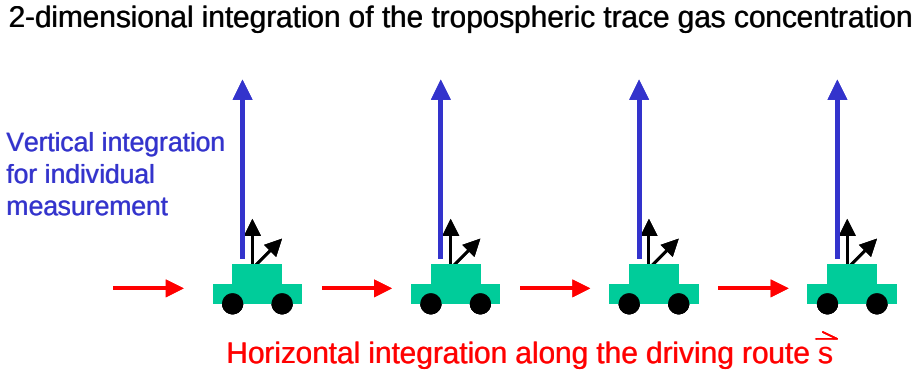

Fig. 1. Form MAX-DOAS observations the vertically integrated tropospheric trace gas concentrations can be determined. If MAX-DOAS observations are performed on mobile platforms, a second integration along the driving route becomes possible (indicated by the blue arrows). The black arrows indicate the viewing directions of the MAX-DOAS instrument.

AMTD
3, 469–499, 2010

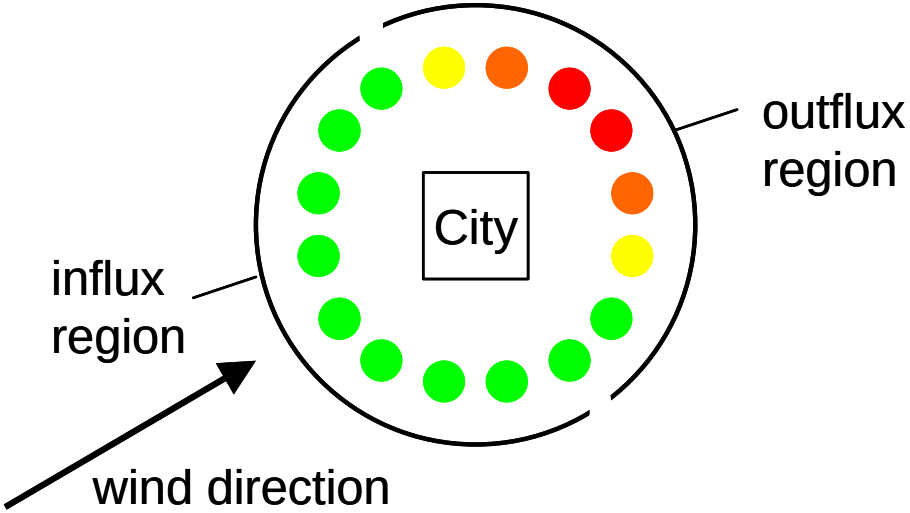

Fig. 2. Example of tropospheric vertical column densities (orange and red colours indicate enhanced values) derived from mobile MAX-DOAS observations around an extended emission source. According to the wind direction a part of the observations characterises air masses entering and a part of them leaving the encircled area.

AMTD
3, 469–499, 2010

Fig. 3. The red rectangle indicates the location of the encircled area around the cities of Mannheim and Ludwigshafen in Southern Germany (see also Fig. 5). (The map was taken from http://www.freeworldmaps.net/europe/germany/political.html.)

AMTD
3, 469–499, 2010

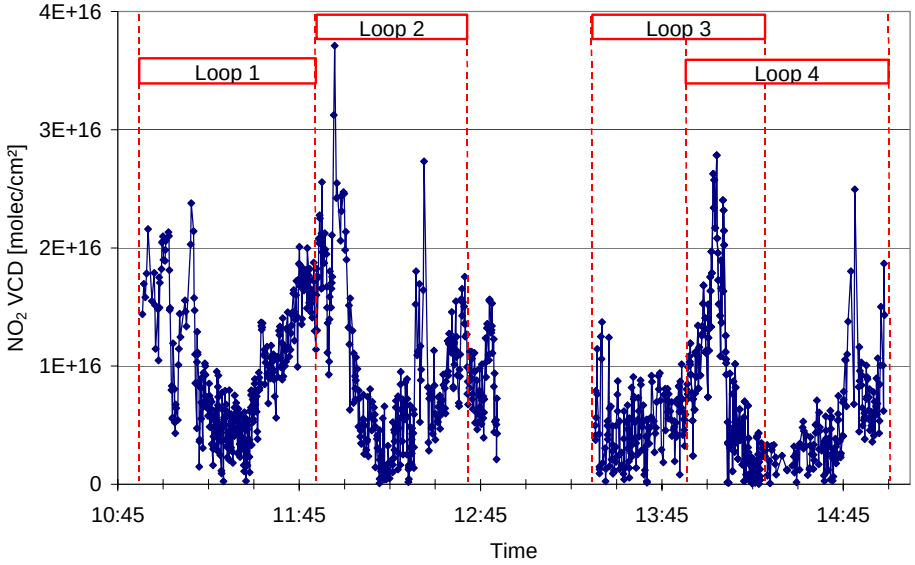

Fig. 4. Time series (4 circles) of the NO_2 VCDs measured around Mannheim-Ludwigshafen area on 24 August 2006.

AMTD
3, 469–499, 2010

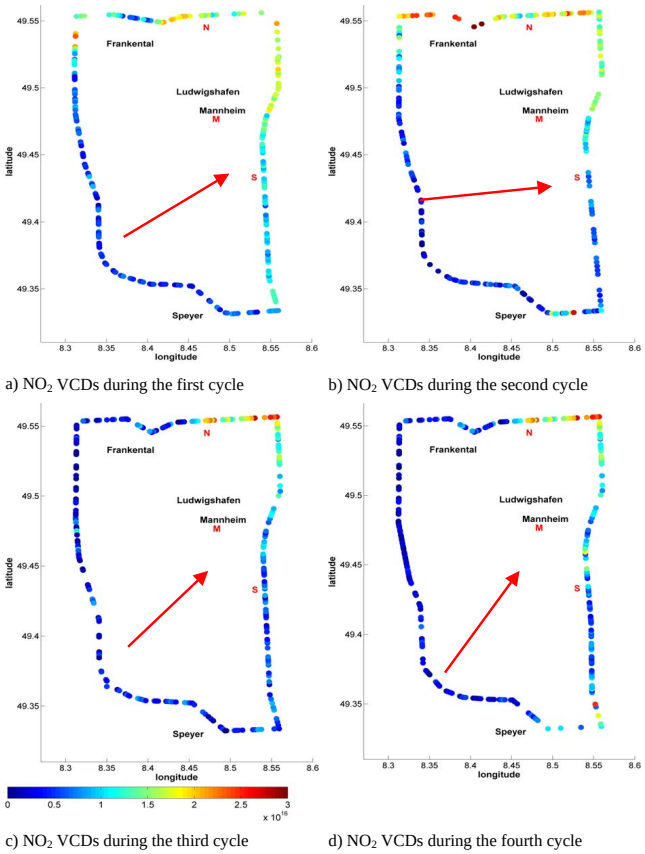

Fig. 5. NO_2 VCDs for the four individual cycles around the Mannheim-Ludwigshafen area on 24 August 2006. The letters "N", "M", and "S" indicate the locations of the in-situ measurement stations Mannheim North, Mannheim Center, and Mannheim South. Arrows indicate the average wind direction.

AMTD
3, 469–499, 2010

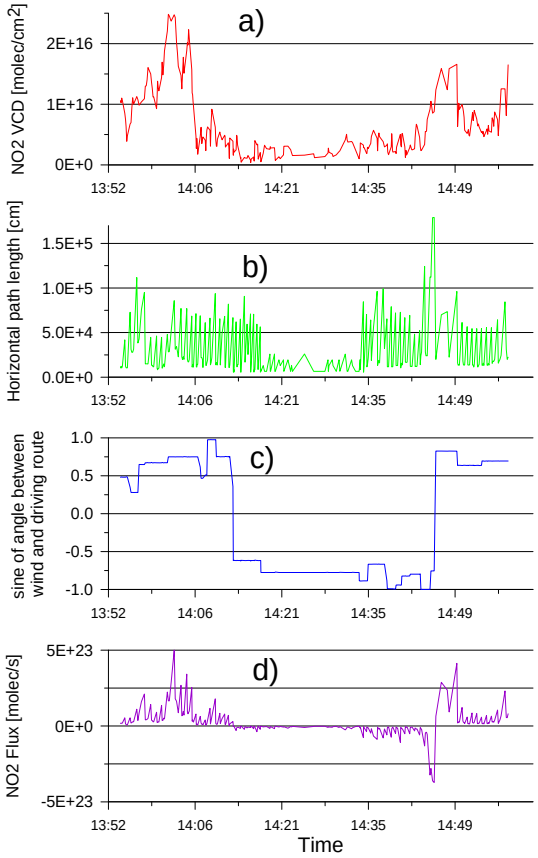

Fig. 6. Different components used for the net flux estimation shown for loop #4 on 24 August 2006. In **(a)** the observed NO_2 VCD are presented. Figure **(b)** shows the driving distance during one observation and **(c)** the sine of the angle between the driving route and the wind direction. In **(d)** the resulting NO_2 flux is shown: negative fluxes indicate import and positive fluxes export from the encircled area.

AMTD
3, 469–499, 2010

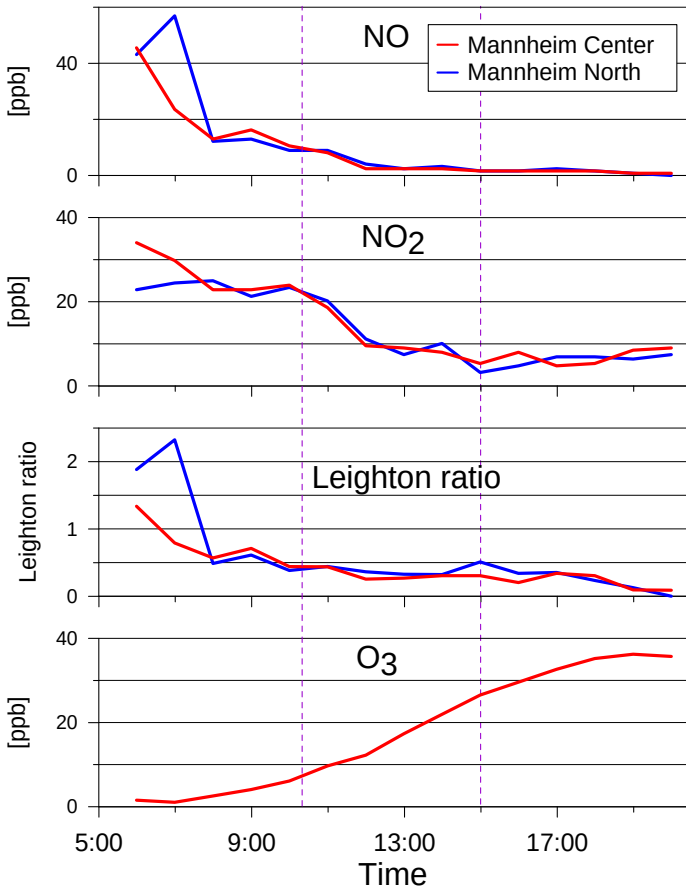

Fig. 7. Diurnal variation of the mixing rations of NO, NO_2, and O_3 for the stations Mannheim North and Mannheim Center on 24 August 2006. Also the Leighton ratio is shown. The vertical lines indicate the start and end times of the Auto MAX-DOAS measurements.

AMTD
3, 469–499, 2010